# <u>Synoptic Meteorology II: Quasi-Geostrophic Height Tendency Equation Examples</u>

The images below from Tom Galarneau's [Real-Time QG Diagnostics webpage] provide data to evaluate the forcing terms to the quasi-geostrophic height tendency equation and thus assess the movement of and amplitude change in the synoptic-scale geopotential height field.

We first focus on a trough in the west-central United States at 0000 UTC 7 February 2019. We see that 500 hPa geostrophic absolute vorticity is maximized in the base of this trough along 110°W (Fig. 1). This would result in the eastward translation of this trough, which is confirmed by Fig. 4.

At both 300 hPa (Fig. 2) and 700 hPa (Fig. 3), warm air advection is found ahead of the trough (at that level) and cold air advection is found behind the trough (at that level). Advection magnitudes are larger at 300 hPa than 700 hPa, and the advection maxima tilt westward with increasing height. Along 110°W, however, which is the axis of the trough at 500 hPa, cold air advection appears to increase upward, particularly from 30-40°N. This is also true west of 110°W. Together, these imply a positive height tendency in the trough's base (a weaker trough) and upstream (an eastward-moving trough). Conversely, cold air advection decreases upward just east of 110°W and warm air advection increases upward further northeast. Together, these imply a negative height tendency associated with the eastward motion of the trough. These insights are confirmed by Fig. 5.

The total forcing is given by the sum of Figs. 4 and 5, as depicted in Fig. 6. Fig. 7 depicts the 500 hPa geopotential height field 12 h later, confirming little to no change in trough amplitude.

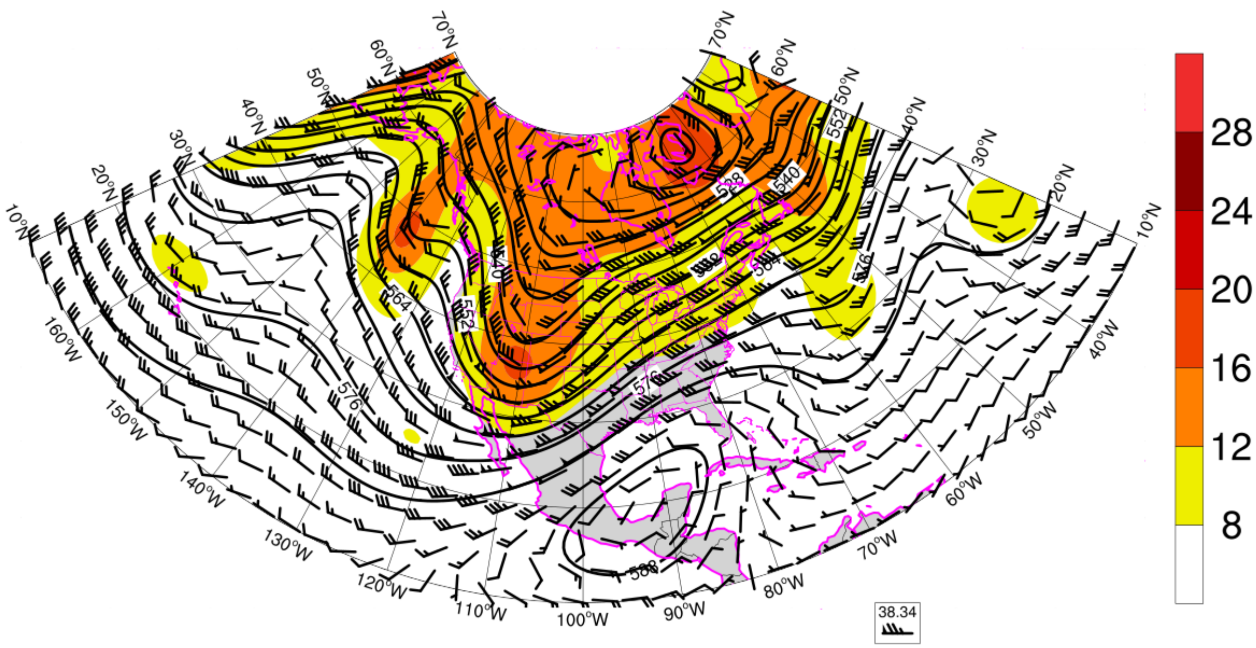


500 hPa Height, Geostrophic Wind, and Geostrophic Absolute Vorticity (smoothed)
0-h CMC Global forecast at 2019020700

**Figure 1**. 500 hPa geopotential height (contours every 6 dam = 60 m), geostrophic wind (barbs; reference barb at lower-right), and geostrophic absolute vorticity (x$10^{-5}$ $s^{-1}$; shaded per the color bar at right) from the 0-h Canadian global model (CMC) analysis at 0000 UTC 7 February 2019.

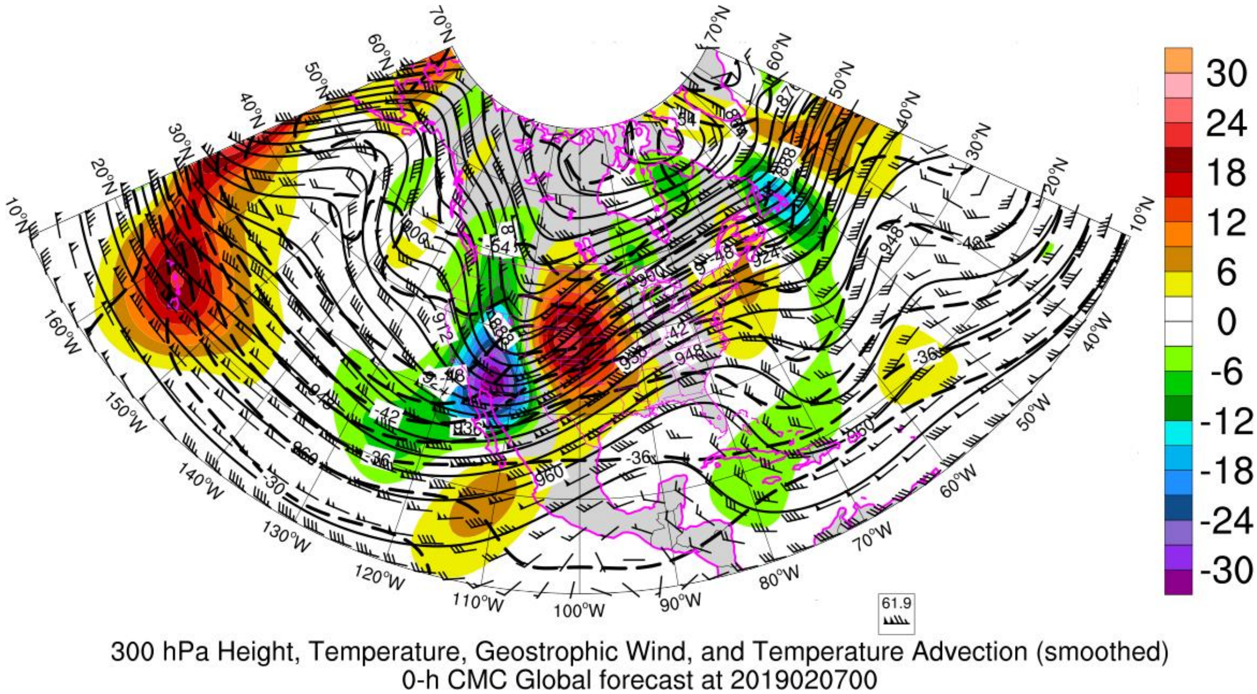


**Figure 2**. 300 hPa geopotential height (solid contours every 6 dam = 60 m), temperature (dashed contours every -3°C), geostrophic wind (barbs; reference barb at lower-right), and temperature advection (°C day$^{-1}$; shaded per the color bar at right) from the 0-h CMC analysis at 0000 UTC 7 February 2019.

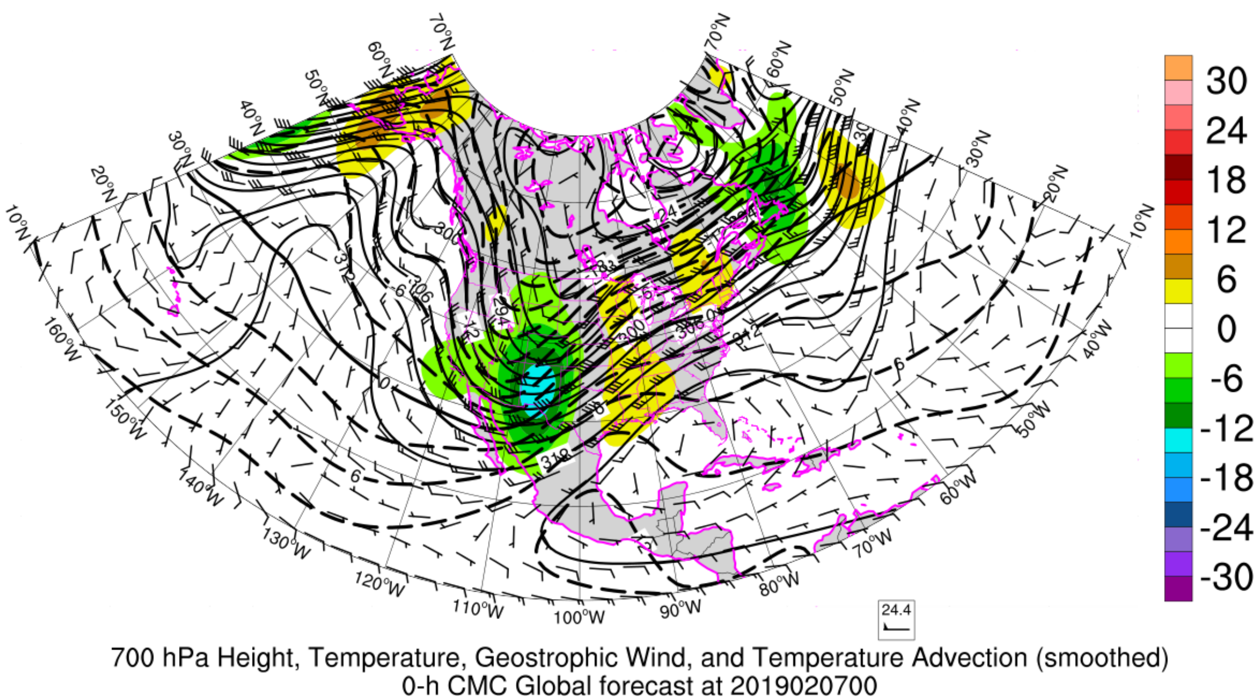


**Figure 3**. As in Fig. 2, except at 700 hPa. Note that the contour interval for geopotential height is 3 dam = 30 m in this figure.

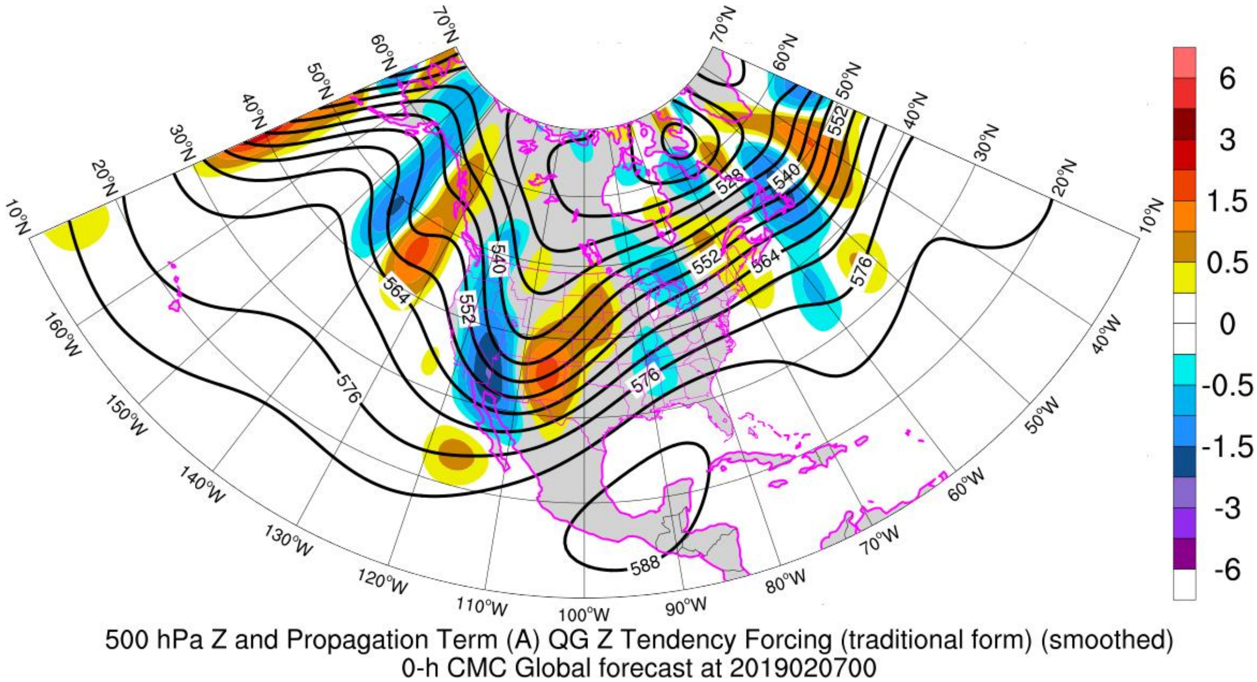


**Figure 4**. 500 hPa geopotential height (contours every 6 dam = 60 m) and geostrophic advection of geostrophic absolute vorticity ("term A"; x$10^{-13}$ $s^{-3}$, shaded per the color bar at right) from the 0-h CMC analysis at 0000 UTC 7 February 2019.

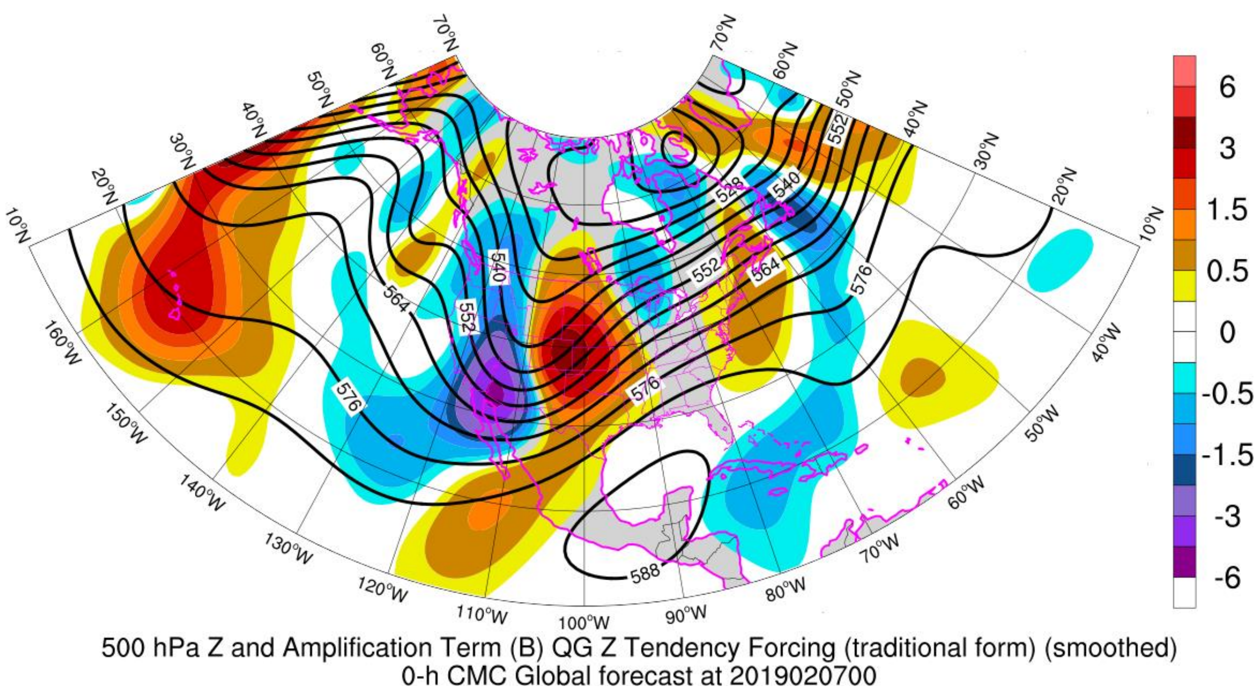


**Figure 5**. 500 hPa geopotential height (contours every 6 dam = 60 m) and differential (700-300 hPa) temperature advection ("term B"; x$10^{-13}$ $s^{-3}$, shaded per the color bar at right) from the 0-h CMC analysis at 0000 UTC 7 February 2019.

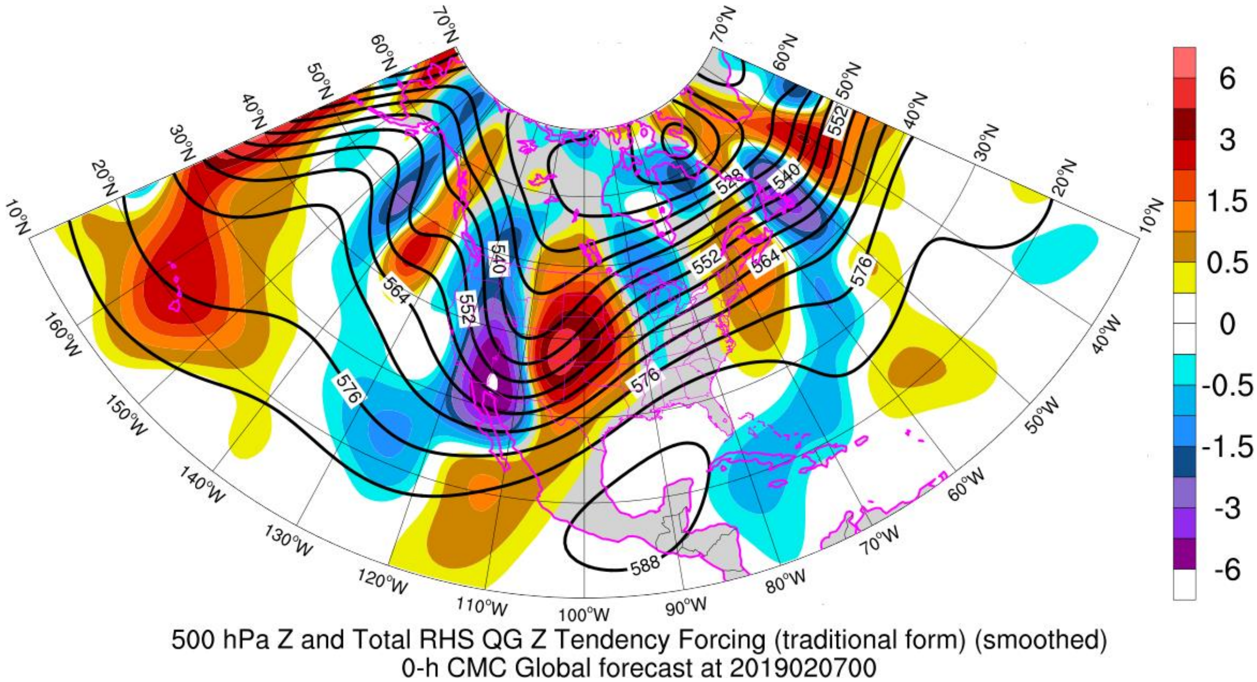


**Figure 6**. 500 hPa geopotential height (contours every 6 dam = 60 m) and the sum of the forcing terms depicted in Figs. 4 and 5 (x$10^{-13}$ $s^{-3}$; shaded per the color bar at right) from the 0-h CMC analysis at 0000 UTC 7 February 2019.

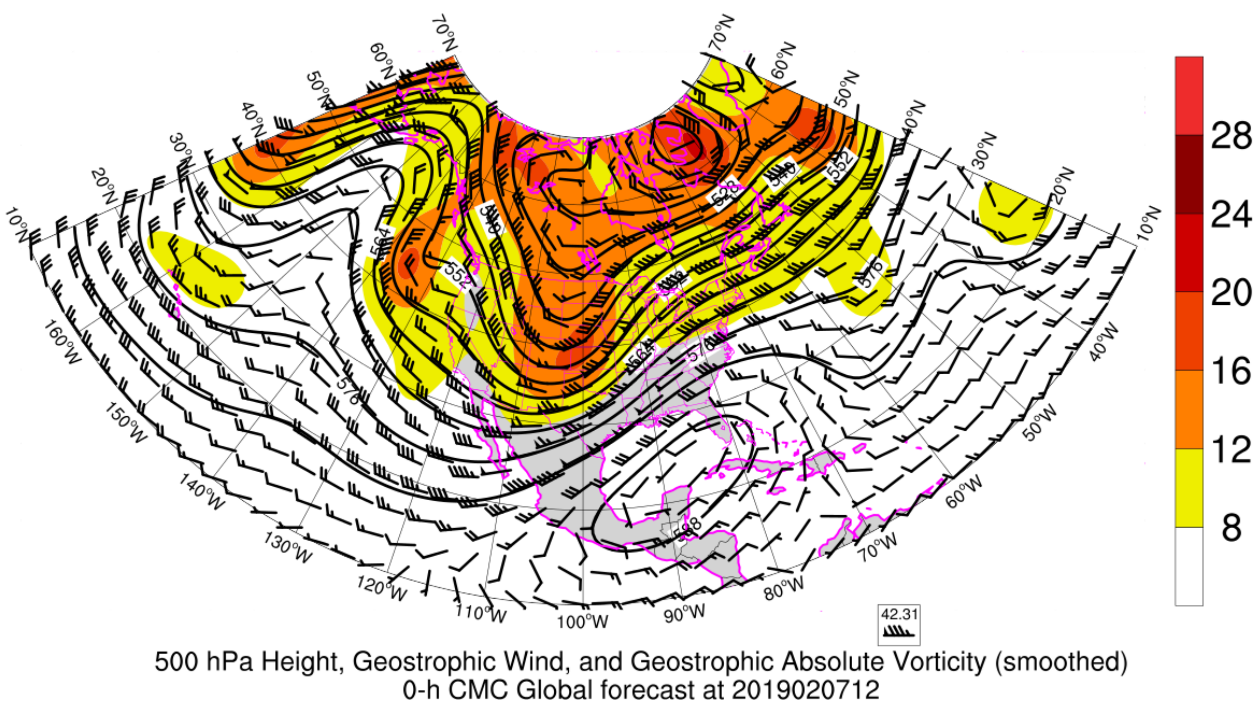


**Figure 7**. As in Fig. 1, except at 1200 UTC 7 February 2019.

We next focus on another trough in the western United States, this one from 1200 UTC 10 February 2019. We see that 500 hPa geostrophic absolute vorticity is maximized in the base to just upstream of this trough from Washington southward through northern California (Fig. 8). This would result in the eastward translation of this trough, potentially with some amplification, as is confirmed by Fig. 11.

For this case, temperature advection at 700 hPa (Fig. 10) is relatively weak in both the base of the trough and its sides. Temperature advection is stronger at 300 hPa (Fig. 9), with warm air advection to the east and cold air advection to the west. These maxima largely lie just west and east of the base of the trough, implying height rises to the west and height falls to the east of the trough, with near-zero differential temperature advection in (and thus no amplitude change of) the base of the trough. This is confirmed by Fig. 12.

The total forcing is depicted in Fig. 13, indicating forcing for the trough's eastward motion and, to much less extent, amplification. Fig. 14 depicts the 500 hPa geopotential height field 12 h later, indicating that the trough deamplifies slightly in this period. This suggests that neglected processes – whether in the QG framework (e.g., friction or diabatic heating) or otherwise (e.g., deformation) – must be at play.

We can also consider the potential impact of diabatic heating – namely, its vertical variation – on this trough. Consider the sounding from Medford, OR, roughly in the trough's base, at 1200 UTC 10 February 2019 (Fig. 15). The atmosphere is saturated from the surface to the tropopause (here, just below 400 hPa), with subsaturated conditions above. We can thus infer clouds and associated diabatic warming below 400 hPa. In general, there is also net radiative cooling atop a cloud deck, as some shortwave radiation is reflected to space and some longwave radiation is emitted toward space. Thus, we can infer weak diabatic cooling above 400 hPa. For an evaluation at 500 hPa, we see diabatic heating becoming less positive/more negative moving upward, from which we expect to see a positive height tendency (i.e., rising heights) in the base of the trough.

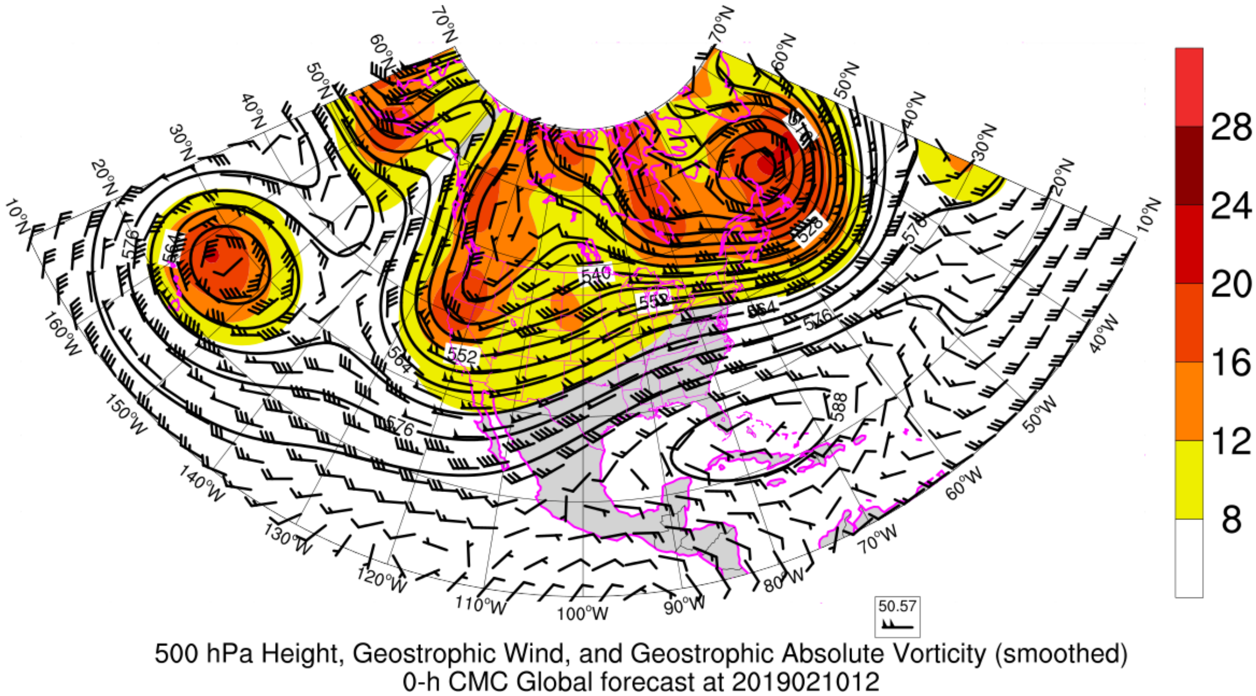


**Figure 8**. As in Fig. 1, except at 1200 UTC 10 February 2019.

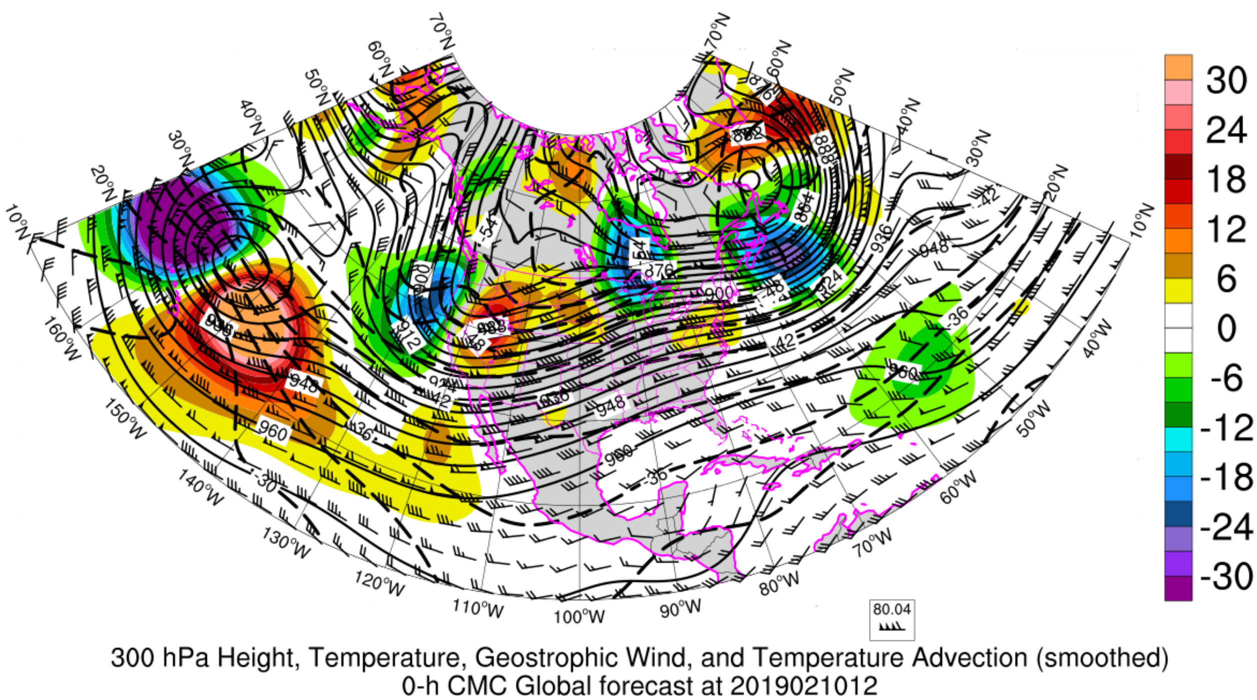


**Figure 9**. As in Fig. 2, except at 1200 UTC 10 February 2019.

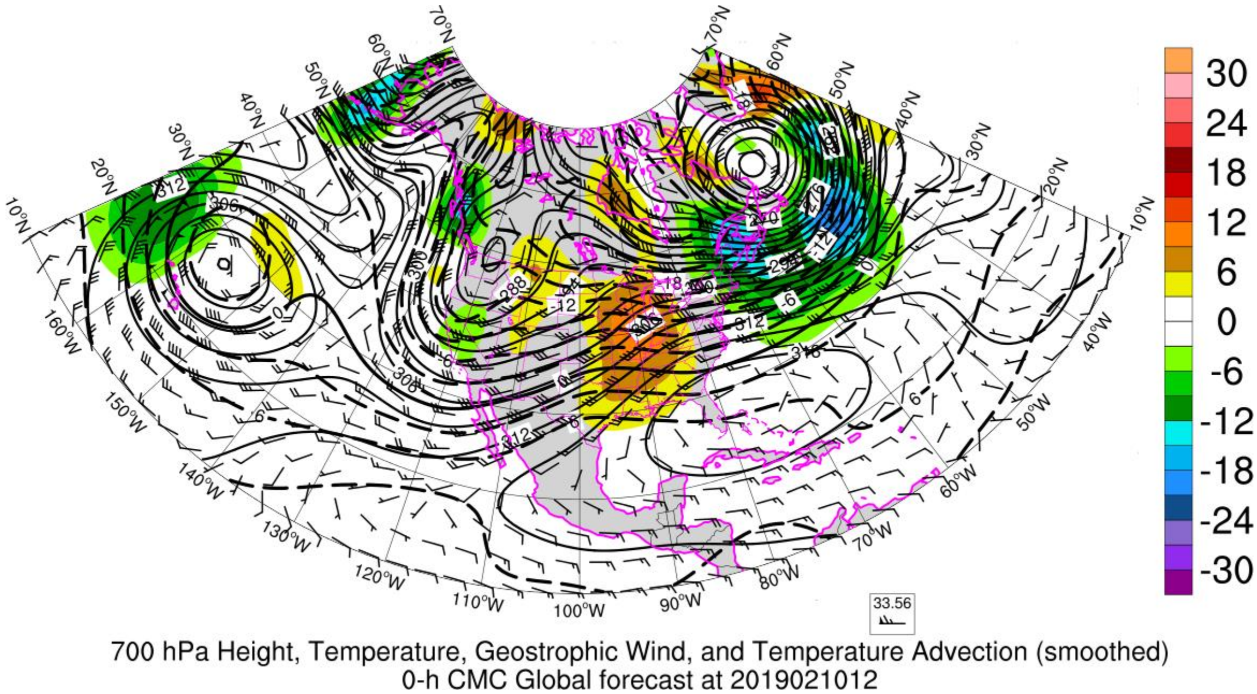


**Figure 10**. As in Fig. 3, except at 1200 UTC 10 February 2019.

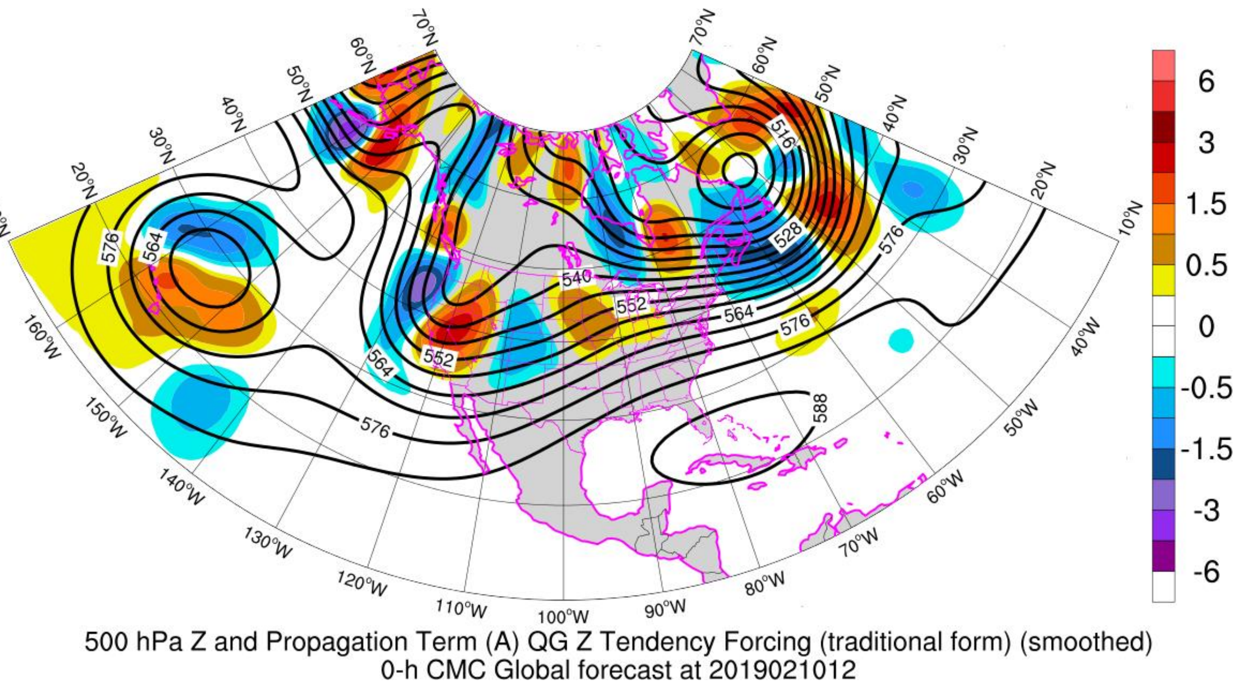


**Figure 11**. As in Fig. 4, except at 1200 UTC 10 February 2019.

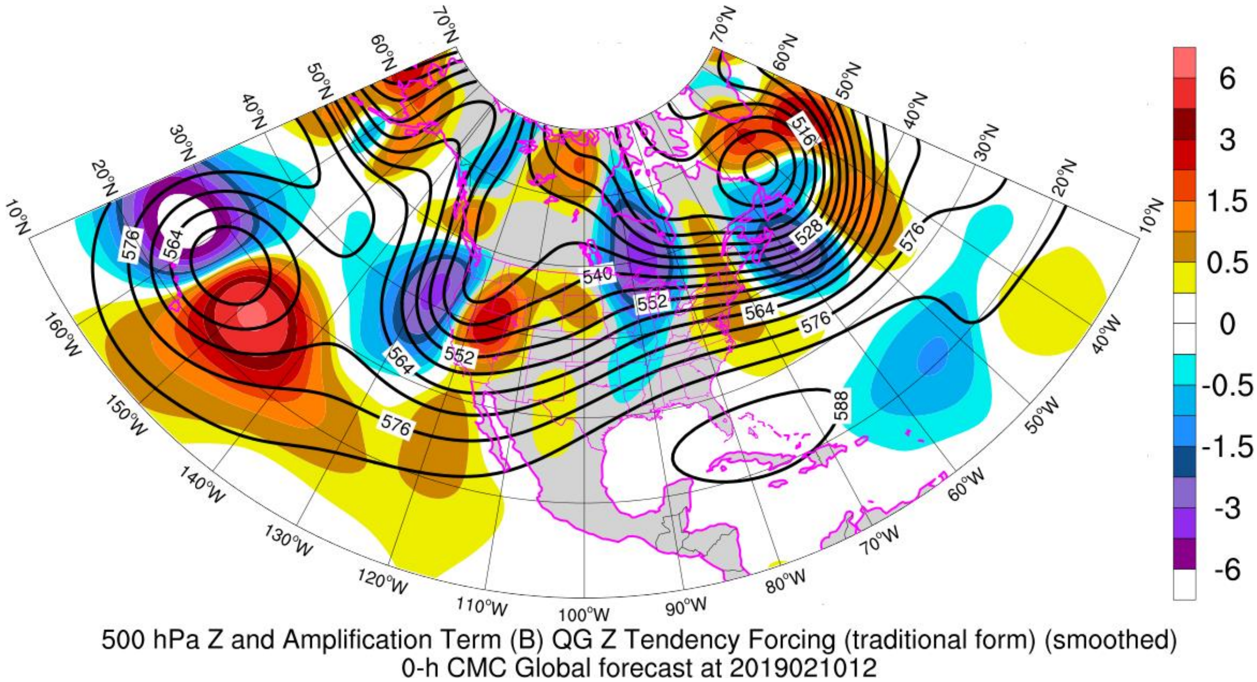


**Figure 12**. As in Fig. 5, except at 1200 UTC 10 February 2019.

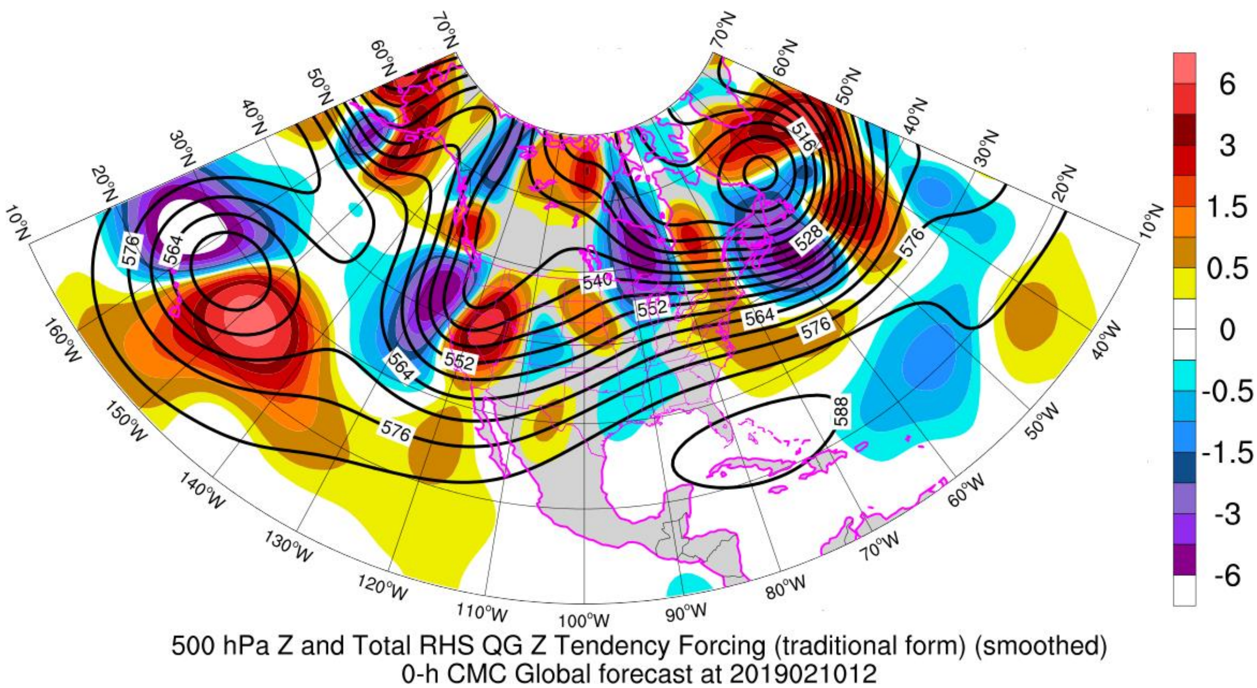


**Figure 13**. As in Fig. 6, except at 1200 UTC 10 February 2019.

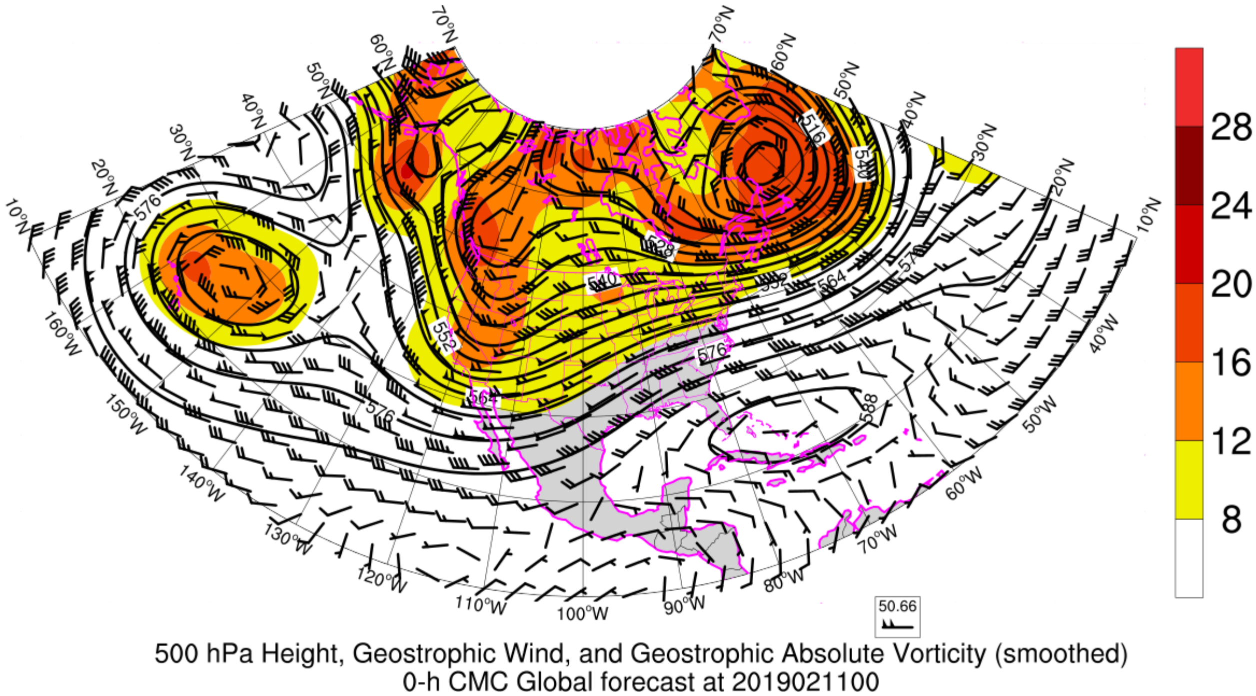


**Figure 14**. As in Fig. 8, except at 0000 UTC 11 February 2019.

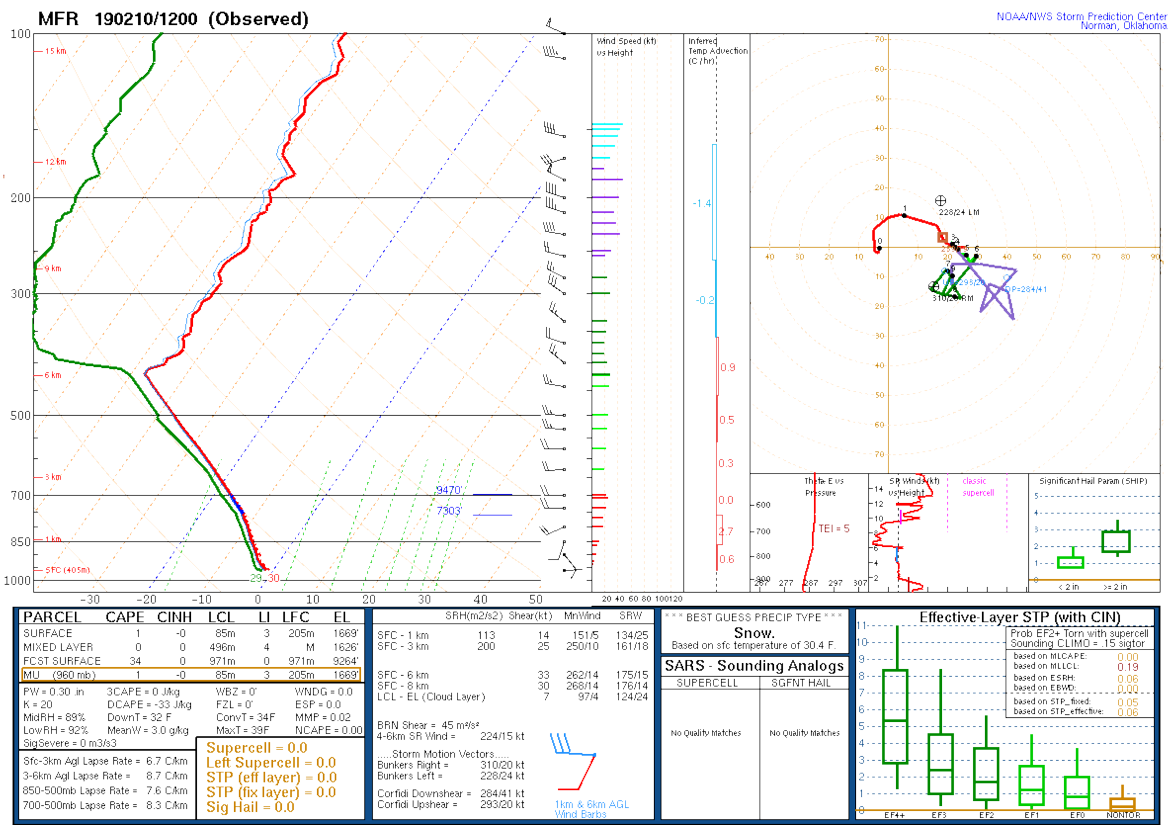


**Figure 15**. Skew *T*-ln *p* diagram from Medford, OR (MFR) valid at 1200 UTC 10 February 2019.